Eur. Phys. J. B **22**, 443–453 (2001)

THE EUROPEAN PHYSICAL JOURNAL B

EDP Sciences

Ab initio studies of the atomic and electronic structure of pure and hydrogenated a-Si

A.A. Valladares[1,a], F. Alvarez[1], Z. Liu[2], J. Sticht[3], and J. Harris[4]

[1] Instituto de Investigaciones en Materiales, UNAM, Apartado Postal 70-360, México, D.F., 04510, Mexico
[2] Molecular Simulations, Inc., 9685 Scranton Road, San Diego, CA, 92121, USA
[3] Materials Design Inc., 5031 Palermo Dr., Oceanside, CA, 92057, USA
[4] Institut für Festköperforschung, Forschungszentrum, Jülich GmbH, 52425, Jülich, Germany

Received 17 May 2001

Abstract. We propose a method to simulate *a*-Si and *a*-Si:H using an *ab initio* approach based on the Harris functional and thermally-amorphisized periodically-continued cells with at least 64 atoms. Hydrogen incorporation was achieved *via* diffusive addition. In preparing samples that may simulate the distributions of atoms in the amorphous materials, simulated annealing calculations were carried out from given starting conditions using short and long time steps. The different time-steps led to samples having distinctly different topological disorder. The radial distribution functions (partial and total) of the resulting samples were calculated and compared with measured distributions; the agreement is very good. These comparisons allowed some tentative conclusions to be made as regards the kind of disorder prevailing in the real samples. In addition, we studied the effect of the topological disorder on the electronic densities of states of the samples; the passivating effect of hydrogen can be observed.

PACS. 71.23.Cq Amorphous semiconductors, metallic glasses, glasses – 71.15.Pd Molecular dynamics calculations (Car-Parrinello) and other numerical simulations – 73.61.Jc Amorphous semiconductors; glasses

1 Introduction

The scientific and technological relevance of *a*-Si, pure and hydrogenated, is well known. Early experimental and theoretical work on the atomic structure of the pure amorphous materials began more than four decades ago. Experimental work on the amorphous phases of pure germanium and silicon evolved in parallel, beginning with the electrolytic approach of Szekely in 1951 [1] and the pioneering efforts of Richter and Breitling in 1958 [2]. Theoretically, the first atomic models of both *a*-Si and *a*-Ge appeared in the literature over thirty years ago. Grigorovici and Manaila [3] and Coleman and Thomas [4] in 1968 suggested structures based on arrangements of closely packed simplified Voronoi polyhedra that have the shape of truncated tetrahedra both eclipsed and staggered 60° about their common bond, leading to rings of five atoms and to boat-like rings of six atoms, as in the carbon and silicon amorphous clusters that we have recently studied [5]. As is well known, fivefold symmetry is not crystallographic and therefore yields an amorphous-like diffraction pattern with broad maxima. The eclipsed configuration with a fivefold symmetry structure is energetically unfavourable in the crystalline phases but occurs in the amorphous form since atomic arrangements with large internal energy can appear in such frozen structures [6].

It was soon realized that such pure structures could not be doped with donors or acceptors because dangling bonds masked the energy gap in the electronic level spectrum, and the search began to find a solution to this problem. Spear and Lecomber [7] discovered that if amorphous silicon is grown in the presence of hydrogen the naturally existing dangling bonds passivate reinstating a clean energy gap and allowing a systematic doping to control the electrical properties. This development radically transformed the study of amorphous semiconductors from an academic subject to a technologically relevant one that has led to the design of devices that are used currently in many applications. Correspondingly, the study of hydrogenated amorphous silicon flourished [8] and became one of the most important subjects in the area of amorphous semiconductors.

In general, advances in amorphous semiconductors have proceeded as a result of experimentation with little concrete input from theoretical simulation. The structures of pure and hydrogenated amorphous silicon have been characterized in particular *via* measurements of the radial distribution functions (RDFs), using X-ray and neutron diffraction. A reasonably consistent picture has emerged for the structure of *a*-Si. However, the situation is less

[a] e-mail: valladar@servidor.unam.mx

satisfactory for *a*-Si:H, where the neutron diffraction experiments needed to probe the hydrogen presence are relatively recent [9] and the information is sparse.

One of the principle difficulties in simulating amorphous structures is the creation of atomic aggregates that resemble the atomic arrangements in the real systems. In principle, one can do this by performing simulated annealing following the conditions that are used in the laboratory to create the amorphous structures. In practice, such simulations are out of range even when force-fields are used because the computational time-step is determined by the movement of individual atoms and is many orders of magnitude smaller than the time scales on which the structures anneal in the laboratory. We propose therefore to create amorphous structures artificially by performing simulations with time steps that are not necessarily 'correct' from the point of view of the actual motions of the atoms (so that the movement of the atoms in our simulations are not necessarily 'real') but do generate different kinds of amorphous structures. That is, the time step in the annealing is used simply to generate, somewhat arbitrarily, a variety of amorphous structures, each of which can be characterized by its RDF. The RDF is $4\pi r^2\rho(r)\mathrm{d}r$, where $\rho(r)$ is the density of particles at point r, and gives the average number of pairs of atoms separated by a distances between r and $r + \mathrm{d}r$. Whereas a given structure generates a well defined RDF, the converse is not the case. Thus, the RDF is not a unique characterization of the atomic arrangement, but nevertheless gives information about this arrangement. By comparing the RDFs generated in simulations, which result from specific well-defined atomic arrangements, with experimental RDFs, information is gained that indicates the probable arrangement of the atoms in the real system. This is the true value of simulations. Simulations start from a known structure which may or may not be close to the true structure of the amorphous material. Experiments start from true structures, but with no knowledge of the detailed atomic arrangement. The RDF is one bridge between the two. Another is the electronic density of states of the structure, which can likewise be measured for the real structure and computed for a known structure [5].

The experimental work of references [10–16] for *a*-Si and references [17] and [18] for *a*-Si:H will be considered in this paper. For hydrogenated silicon, reference [18] reports the only complete study of the total RDF, together with the partials for Si-Si, Si-H and H-H.

A considerable amount of previous work has addressed the atomic structure of *a*-Si, and, more recently, *a*-Si:H. Attempts to generate reasonable atomic topologies can be classified *via* two extremes: i) calculations that are carried out in samples that are constructed essentially "to order" by switching bonds and adjusting dihedral angles, and that use *ad hoc* classical, parameter-dependent potentials constructed for the specific purpose of describing them; and ii) quantum methods, parameterized and *ab initio*, that can deal from the outset with the thermalization processes that generate the amorphous structure, and the study of their corresponding electronic structure.

A particularly nice example of type i) is the computationally cost-effective work performed with classical techniques in very large supercells of *a*-Si that contain tens of thousands atoms (see Ref. [19] and work cited therein). This methodology is powerful provided the interactions between the atoms in the materials (force-fields) are reasonably adequately described. This requirement restricts the generality of the method, since the interactions are not transferable to other amorphous materials. New force-field parameters and potentials must be generated for each new material using either comparison with known data from experiment or from *ab initio* calculations. It is notoriously difficult to generate force-fields and model potentials with any degree of universality so that, even if the RDF is well described this does not necessarily mean that other properties are well described [20]. There is always a limit to which model interactions can mimic properties that are inherently quantum mechanical.

Quantum methods have answered some of the unsolved questions left by the classical approaches, and are themselves of several kinds. For example, there has been some interesting work done using tight binding methods for pure silicon [21], where a transferable model is found by fitting the energies of silicon in various bulk crystal structures and examining functional parameterizations of the tight binding forms. For hydrogenated silicon a transferable model has also been found by fitting parameters to silane [22]. At the other end of the scale are *ab initio* methods that attempt to answer all the questions from first principles and are generally applicable without adjustment of parameters. These methods are very demanding in computer resources and so are limited to handling relatively small amorphous cells. It remains an issue as to how generally and how accurately an *ab initio* method that uses a reasonably sized supercell can describe the properties of amorphous materials. The present work addresses this issue for amorphous silicon and for hydrogenated amorphous silicon.

2 Antecedents

Because of their technological importance there has been a great deal of work on the systems we study. In this section we mention some of the work that appears to us to be most relevant to our own. Most of these calculations stem in one way or another from the original work of Car and Parrinello [23] (see [23] through to [28]) and from Buda *et al.* [29] (see [29] through to [31]). More recent work is described in the papers of Lee and Chang [28] for *a*-Si and Tuttle and Adams [31] for *a*-Si:H. These calculations all approached the structural problem by generating amorphous cells using first-principles quantum methods.

More than a decade ago Car and Parrinello [23] performed the first *ab initio* molecular dynamics (MD) study in an fcc cell with 54 atoms of silicon using their plane wave MD method. In their approach a non-local pseudopotential was used together with the parameterized local density (LDA) form of Perdew and Zunger for the

exchange-correlation effects. They obtained good agreement with the experimental RDF of *a*-Ge, rescaled to simulate *a*-Si, up to the second radial peak and argued that because of the size of the cell used distances larger that 6 Å could not be studied. They pointed out that the comparisons of simulated and experimentally determined atomic structures should be carried out with care in view of the large number of defects that are generated. A typical simulation was started above the melting point, at about 2,200 K, and the liquid was allowed to equilibrate for $\approx 0.7 \times 10^{-12}$ s before it was quenched down to $\approx$ 300 K at a cooling rate of $\approx 2 \times 10^{15}$ K/s. During the initial quenching the volume of the cell was gradually increased to 1080 $Å^3$, the crystalline value. This technique of quenching from the melt has been used in subsequent work although handling the transition from the liquid to the amorphous phase is not an easy task since a volume change has to be dealt with. In addition, liquid silicon is metallic with an average coordination number of between 6 and 7 and the quenching preserves some of this over-coordination.

Drabold *et al.* [24] use the density functional local density approximation (DFT-LDA) molecular dynamics approach developed by Sankey *et al.* [32]. This method is based on a simplification of the Kohn-Sham equations suggested by Harris [33]. Drabold *et al.* used a 64-atom simple cubic cell in the diamond structure with a single vacancy and generated an "incompletely melted" sample by heating this system up to 8,000 K. The free evolution of the cell then results in the system acquiring a highly disordered liquid-like structure before final quenching to a solid. Although a detailed comparison was not given, the resulting RDF were found to agree with measured distributions. Four coordination defects were found, two dangling and two floating bonds, for appropriate values of the rate of free evolution of the cell. After annealing at 300 K only two defects survived.

A more complete report of the Car and Parrinello results is given in Stich *et al.* [25], where a cooling rate of of 10^{14} K/s was used starting from the melt. The slower cooling rate generated a tetrahedral network that nevertheless contains several coordination defects as well as a large fraction of distorted bonds. Annealing at 900 K reduced the number of defects and the RDF displayed a two peak structure that align reasonable well with the first two peaks of experiments. The study performed by Drabold *et al.* was extended [26] to the 216 atom periodic supercell of Wooten, Winer and Weaire [27] and a more complete analysis of the relationship of structural defects, spectral defects and interatomic distances was carried out. Lee and Chang [28] performed *ab initio* simulations on a 64-atom silicon cell and quench incompletely melted samples as in reference [24], but they find that the third peak of the RDF practically disappears, and that more dangling and floating bonds occurred than in previously generated samples from liquid-quenched simulations, and than in the samples generated by Drabold *et al.* [24].

Theoretical work on *a*-Si:H has been less abundant because the experimental RDF results are limited and it is more difficult to model interactions of H and Si and cope with the time steps needed for computer simulations of hydrogen diffusion. In addition, the strong dependence of the *a*-Si:H structure on deposition conditions together with the chemical reactivity of hydrogen needs to be taken into account. Also, the role of zero point energy is not a priori obvious. Basically, this system requires quantum mechanical, *ab initio* methods such as the work reported in references [29–31].

The plane wave MD Car-Parrinello method was first applied to amorphous hydrogenated silicon by Buda *et al.* [29] using a cubic cell of 64 silicons and 8 hydrogens (11% concentration). These authors start out with a liquid material containing both silicon and hydrogen atoms that is rapidly quenched, maintaining a density equal to the value of the crystalline material. They report only partial distribution functions and, as is the case in many simulations, the H-H RDF is in poor agreement with neutron scattering data.

The DFT-LDA approach of Sankey and co-workers was applied to this material by Fedders and Drabold [30] using several cells based on a two-defect 63 silicon atom supercell that was constructed in previous work [24,26]. The hydrogen was introduced into the amorphous silicon sample by hand so that the H-atoms are located near (1.5 Å), the corresponding dangling bond. To eliminate the strained bond defects they removed the silicon considered to be the center of the strain defect and put H atoms near the 4 dangling bonds. Subsequent relaxation allowed the hydrogens to be trapped by the dangling bonds. Fedders and Drabold [30] do not report any RDF, total or partial. Tuttle and Adams [31] also use the Harris functional in the DFT-LDA code developed by Sankey *et al.* and apply it to a cell of 242 atoms with 11% hydrogen. They generated their structures from a liquid at $\approx$ 1800 K, which they quench to produce an amorphous sample at 300 K. Since they were not concerned with real time dynamics, they set the mass of hydrogen equal to the mass of Si, thereby allowing the use of a large time step in the annealing process (4 fs). However, this means that the RDFs could not reflect real diffusion processes of the hydrogens in the cell, and correspondingly only the Si-Si and the Si-H RDFs are reported. A significant percentage of defects with only 90% of the silicon being fourfold coordinated was found, as is usually the case when liquid samples are quenched.

Although the tight binding method is not obviously applicable to silicon [26], the approach has been used to study dangling and floating bonds [34] and the energetics of defects. Fedders [35] found that tight binding gives surprisingly good results for the energy eigenvalues and the degree of localization of the defect states if some radial dependence is included in the hopping matrix elements. Colombo and Maric [36] reported the first tight-binding molecular-dynamics simulation of the defect-induced transition from crystal to amorphous in crystalline silicon. In particular, two recent ones are specially relevant for the present work: Yang and Singh [37] find that the total average energy per silicon atom is a minimum when the hydrogen concentration is in the range 8–14%, the optimum

experimental range found. Klein *et al.* [38] report a H-H RDF closer to experimental results than previous work. Both studies start out from liquid samples that are fast quenched to generate the hydrogenated amorphous silicon and therefore, as in all other cases, a large percentage of defects, floating or dangling bonds, are naturally created. For a recent account of the state of the art of tight binding methods see reference [39], where both parameterized and *ab initio* approaches are considered.

3 Present method

In the present work we propose to generate samples of both *a*-Si and *a*-Si:H using a new approach that amounts to controlling the number and kind of coordination defects by tuning the time step used in the annealing process. As in previous computations, the physical process the system undergoes during the annealing is artificial and is carried out merely in order to generate a variety of amorphous-like structures. The computations were performed using the code *FastStructure* [40], a DFT code based on the Harris functional, which generates energies and forces faster than traditional Kohn-Sham functional methods [41]. We use the LDA, with the parameterization of Vosko, Wilk and Nusair (VWN) [42] in all simulations. The calculations are performed on an all electron basis, within the frozen core approximation. The valence orbitals were described *via* a minimal basis of 'finite-range' atomic orbitals with a cut-off radius of 5 Å, (compare to values of ≈ 2.6 Å used by Sankey *et al.*). This value for the cut-off was chosen as a compromise between cost and accuracy. The computation scales with a high power of the cut-off radius, because the time-limiting factor is the number of three-center integrals that have to be carried out. The forces are calculated using rigorous formal derivatives of the expression for the energy in the Harris functional, as discussed by Lin and Harris [43]. Three-center integrals were performed using the weight-function method of Delley [44] (with correction for the dependence of the mesh on the nuclear coordinates). The physical masses of hydrogen and silicon are used throughout and this allows realistic diffusive processes of the hydrogen atoms to occur in the supercell. Simulations were carried out using the default time step of FastStructure, given by $\sqrt{m_{\min}/5}$, where $m_{\min}$ is the value of the smallest mass in the system: 2.44 fs for pure silicon and 0.46 fs for hydrogenated silicon, but also for much larger values of the time steps: 10 fs for *a*-Si and 2 fs for *a*-Si:H.

It is clear from previous work that quenching from a melt or from partially melted samples generates structures that resemble only poorly the local arrangement of atoms in the amorphous material; therefore we took a different route. Our procedure, like the ones mentioned above, is not designed to reproduce the way an amorphous material is grown, but has the objective of generating an amorphous sample that would represent adequately the ones obtained experimentally. We amorphisized the crystalline diamond structure with 64 silicon atoms in the cell (a crystalline density of 2.33 g/cm^3) by slowly heating it from 300 K to 1,680 K, well above the glass transition temperature and just below the melting point, in 100 steps of $t = 2.44$ fs, and immediately cooled it down to 0 K in 122 steps of 2.44 fs. The same procedure was followed with a time step of $t = 10$ fs. The heating/cooling rates were 5.66×10^{15} K/s for $t = 2.44$ and 1.38×10^{15} K/s for $t = 10$ fs, comparable to values used in reference [23]. The atoms were allowed to move freely within each cell of volume (10.8614 Å)^3 with periodic boundary conditions. Once this first stage was complete, we subjected each cell to annealing cycles at 300 K (below microcrystallization [8]) with intermediate quenching processes.

Table 1. Relative starting positions of the hydrogen atoms in the amorphous cells.

H1	(1/4, 1/4, 1/4)
H2	(3/4, 1/4, 1/4)
H3	(3/4, 3/4, 1/4)
H4	(1/4, 3/4, 1/4)
H5	(1/2, 1/4, 1/2)
H6	(3/4, 1/2, 1/2)
H7	(1/2, 3/4, 1/2)
H8	(1/4, 1/2, 1/2)
H9	(1/4, 1/4, 3/4)
H10	(3/4, 1/4, 3/4)
H11	(3/4, 3/4, 3/4)
H12	(1/4, 3/4, 3/4)

For *a*-Si:H we implemented two different procedures. First, we used the amorphous pure silicon cell generated above with a time step of $t = 2.44$ fs and then expanded it to a volume of (11.0620 Å)^3 to reproduce the experimental density, 2.2 g/cm^3, of the hydrogenated structure. Second, we amorphisized a previously expanded crystalline cell of 64 silicon atoms with the same volume of (11.0620 Å)^3 using a 10 fs time step. We then placed the 12 hydrogens evenly distributed throughout the amorphous cells. The starting locations of the hydrogen atoms in the cell are given in Table 1. The hydrogenated sample was then subjected to annealing cycles using a time step of $t = 0.46$ fs for the first cell (the 2.44/0.46 cell), and $t = 2$ fs for the second (the 10/2 cell). The annealing cycles consist of two cycles of 50 steps at 300 K for the large time step sample and one cycle of 200 steps for the small time step sample, with inbetween quenches down to 0 K, to allow the hydrogens to diffuse and move in the cells. This gives a concentration of hydrogen of practically 16%, adequate to compare with existing experimental results.

Once the atomic structures were constructed and their respective RDFs obtained, we analyzed their electronic density of states at the Γ-point of the Brillouin Zone, as is common in the field. We carried out energy calculations using both *FastStructure* and the full Kohn-Sham DFT approach (Hohenberg and Kohn [45] and Kohn and Sham [46]) implemented in the *ab initio DMol3* commercial code [47] to obtain the energy levels and DOS curves of the final amorphous atomic structures, using the LDA

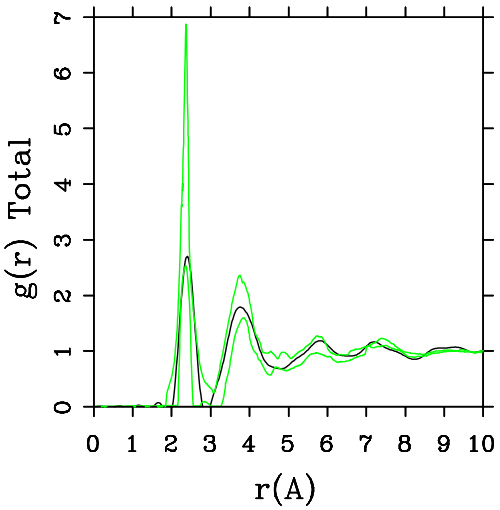

Fig. 1. RDFs for *a*-Si. The lighter lines are the experimental upper and lower bounds (Refs. [10–16]). The dark line is our simulation for 10 fs and it shows four well defined peaks.

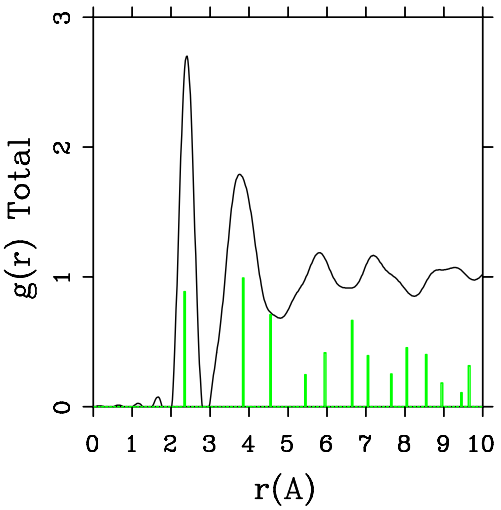

Fig. 2. The RDF for *a*-Si (dark line) has four well defined peaks that are generated by several crystalline peaks (lighter vertical lines).

approximation. In *DMol3* we used a double numerical basis set that includes *d*-polarization of the atoms (DNP) and the frozen inner core orbitals approximation along with a medium grid for the calculation of integrals. The SCF density parameter that specifies the degree of convergence for the LDA density was set at 10^{-6}.

4 Results and discussion

In this section we discuss the results and conclusions we draw from our simulations. We focus first on the atomic structure that the simulation protocols we have carried out generated and show comparisons of their partial RDFs with measured distributions. Then we discuss the electronic structure to which these atomic arrangements give rise with special emphasis on the kinds of defects found and the influence of these defects on the electronic density of states.

4.1 The atomic structure

Of the two simulations carried out for *a*-Si, the one performed at the 'physical time step' of 2.44 fs gave an RDF that resembled the measured distributions only poorly. The computed RDF showed a degree of disorder not compatible with the physical system. Presumably, this disorder would anneal out if we were able to continue the simulation for a considerably longer time period. In an attempt to shortcut the need for very long computation times, and bearing in mind that our goal is simply to generate an amorphous structure, we tried increasing the time interval between steps arbitrarily to a value of 10 fs. This is too large for the motions of the atoms to be physically reasonably represented, but does give the system more opportunities to explore the energy surface.

The RDF generated by this second simulation is shown in Figure 1 along with upper and lower bounds for the experimental RDFs as taken from the literature (Refs. [10–16]). The peak structures of the computed and measured RDFs are similar, with two distinct peaks at smaller values of r and weaker maxima around $r = 5.7$ and 7.2 Å.

The relation between the RDF for the amorphous and purely crystalline materials is shown in Figure 2. The first two peaks of the amorphous structure line up clearly with the first two crystalline peaks, showing that both systems display similar short-range order. However, thereafter, there is no direct correspondence between the peak structures of the amorphous and the crystalline distributions. We take the agreement between the computed and measured RDFs shown in Figure 1 to imply that the simulation procedure we followed generated a structure which is truly characteristic of the amorphous material. Whether this would be generally true if the same procedure were applied to other, similar materials remains, of course, an open question.

The two Si systems generated were then used as starting points for constructing cells of hydrogenated amorphous silicon. Although the short simulation gave a silicon structure whose RDF is not in good agreement with experimental RDFs for the amorphous material, it is not necessarily a worse starting point for preparing a hydrogenated sample. Hydrogen atoms tend to decorate dangling bonds, and the shorter time simulation generated more defects. Thus, both configurations of atoms were used in attempting to generate an acceptable hydrogenated structure. We performed one simulation with each *a*-Si sample, retaining consistency with the time interval between steps. Starting from the 2.44 fs sample, we used the physical time step of 0.46 fs for the subsequent evolution. We refer to the resulting structure as 2.44/0.46. With the second simulation, performed using the 10 fs *a*-Si as starting point, we used a

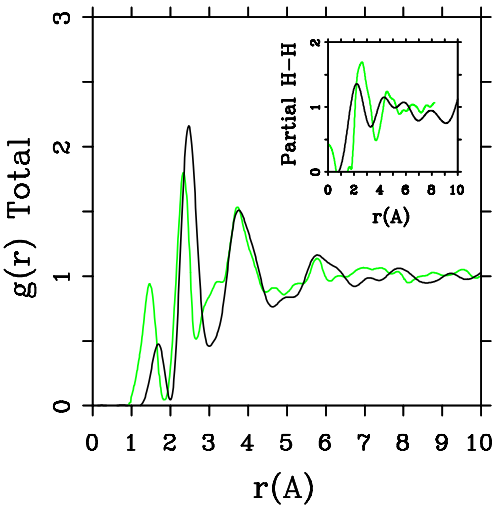

Fig. 3. Direct comparison of the simulated total RDF and H-H RDF (Inset) for *a*-Si:H (dark lines) to the experimental results (light lines) for the 2.44/0.46 fs cell.

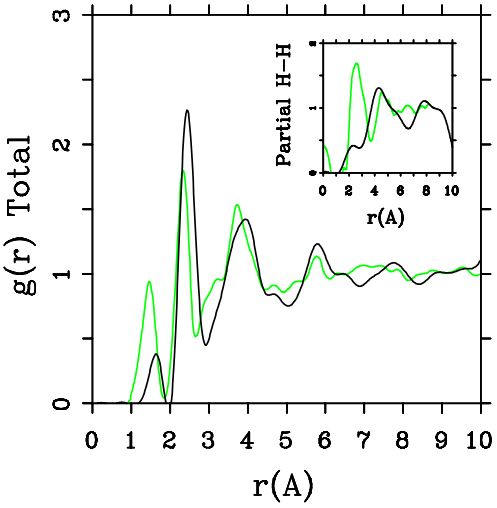

Fig. 4. Direct comparison of the simulated total RDF and H-H RDF (Inset) for *a*-Si:H (dark lines) to the experimental results (light lines) for the 10/2 fs cell. The peak due to molecular hydrogen is not shown.

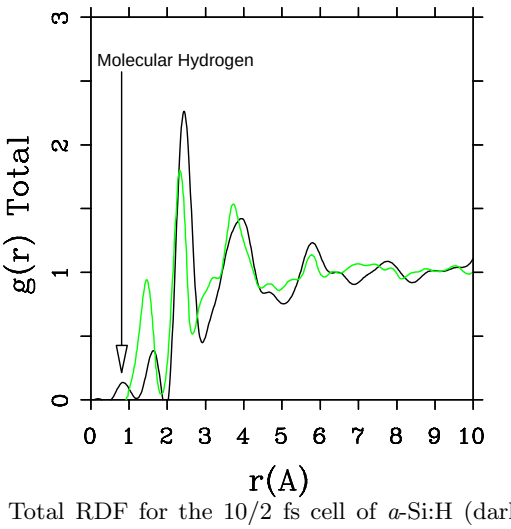

Fig. 5. Total RDF for the 10/2 fs cell of *a*-Si:H (dark line) that shows the presence of molecular hydrogen, compared to the experimental results (light line).

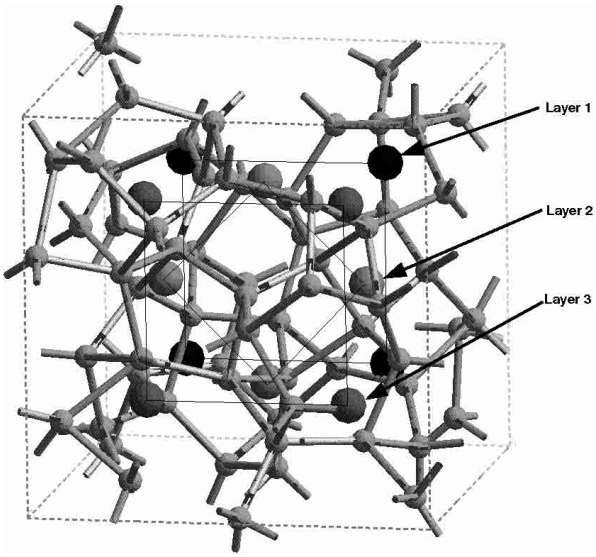

Fig. 6. Starting positions of the 12 hydrogens placed within the amorphous cells of pure silicon.

2 fs time step for subsequent evolution and will be referred to as 10/2.

One important difference between the two simulations was the formation of 'molecular hydrogen' in the 10/2 case. The reason for this is the greater degree of Si coordination in this sample, which leaves insufficient opportunities for the H-atoms to bond to silicons. In the 2.44/0.46 case, the defect/dangling bond density was sufficiently high that all hydrogens could find good bonding locations in a Si environment. In general, the 2.44/0.46 gave a better overall description of the observed H-H partial RDFs than the 10/2 simulation. Direct comparisons in the two cases are shown in Figures 3 and 4, where in the latter case the peak due to di-hydrogen has been removed.

While both simulations represent the main features of the measured total RDF reasonably, the H-H partial RDF is much better represented in the 2.44/0.46 simulation. The experimental data of Bellissent *et al.* [17] are better reproduced by the originally highly defective sample of *a*-Si with added hydrogen. The experimental features observed for $r \approx 0$ are spurious [17]. The presence of di-hydrogen in the 10/2 simulation is illustrated in the RDF in Figure 5. The 'molecular' hydrogen peak appears at an interatomic distance of 0.875 Å, very close to the molecular radius of 0.86 Å found for hydrogen in crystalline silicon [48]. In Figure 6 we show the locations in the cell where the hydrogen atoms were placed at the outset of the simulation.

Defining a dangling or a floating bond in terms purely of the atomic structure of a defect is to some extent arbitrary since one has to choose some interatomic cut-off distance to establish whether a bond exists or not between a given pair of atoms. Drabold *et al.* [24], *e.g.*, chose an interatomic distance of 2.7 Å. Lee and Chang [28] use

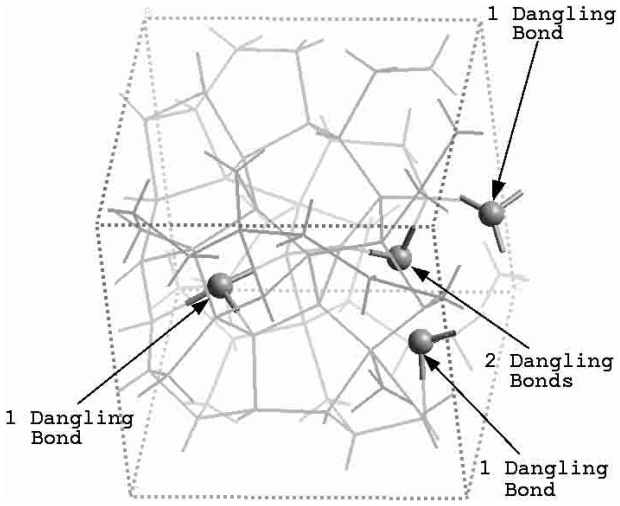

Fig. 7. Amorphous silicon 2.44 fs cell that shows the existence of 5 dangling bonds. A cutoff radius of 2.815 Å was used, below which the total number of first neighbors is 4.

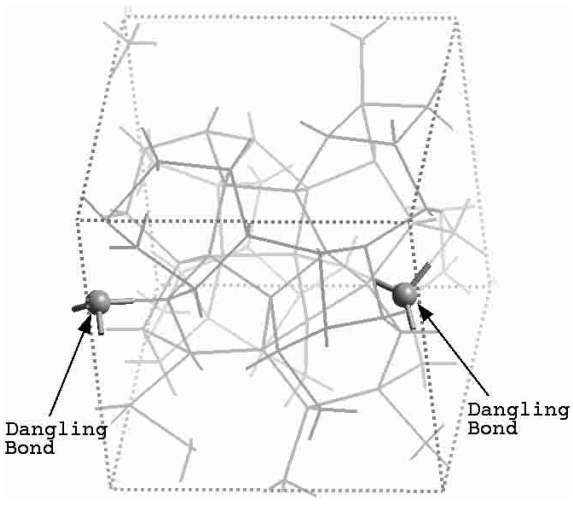

Fig. 9. Amorphous silicon 10 fs cell that shows the existence of 2 dangling bonds. A cutoff radius of 2.743 Å was used, below which the total number of first neighbors is 4.

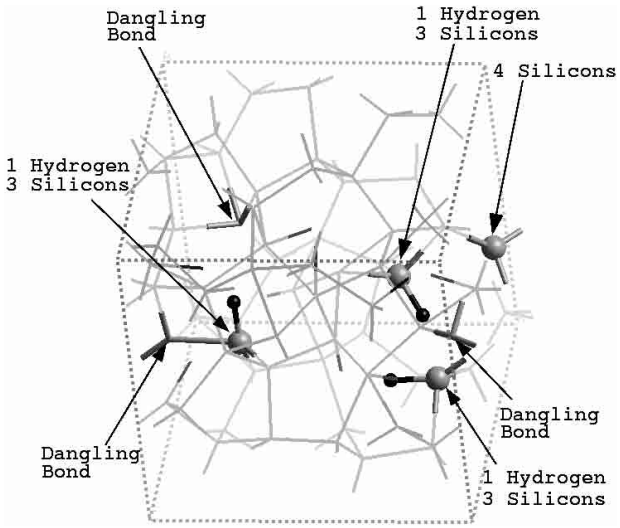

Fig. 8. Hydrogen addition to the 2.44/0.46 cell passivates 3 dangling bonds and 2 other are passivated by silicons but 3 new ones appear; 11 new floating bonds are formed.

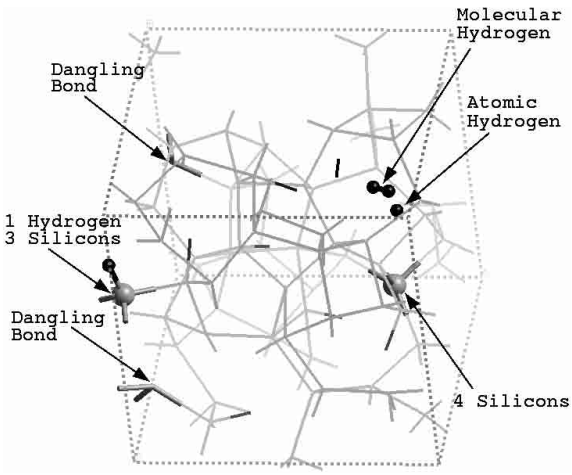

Fig. 10. Hydrogen addition to the 10/2 fs cell passivates all dangling bonds (2) and 2 new ones appear plus 3 floating bonds. The molecular and atomic hydrogens are indicated.

the distance at which the minimum of the RDF occurs, 2.73 Å, which leads to an average number of first neighbors in the amorphous cell of 3.9. If instead one used the minimum value of the RDF of Fedders *et al.* [26], $\approx 1.2 \times 2.35 = 2.82$ Å, the number of defects in the simulations of Drabold and co-workers would have changed significantly. Nevertheless, one needs to settle on some recipe and the one we use for *a*-Si is that the cut off corresponds to a distance below which the total number of neighbors is 4; *i.e.*, the area under the RDF curves between zero and the cut off radii is 4. These values fall within the region where the total RDF has its first minimum: 2.815 Å for the 2.44 fs cell and 2.743 Å for the 10 fs cell.

Figures 7 to 10 depict four structures that display the passivation of dangling bonds in the pure amorphous silicon samples due to hydrogenation. Figures 7 and 9 show the dangling bonds of the amorphous silicon samples prior to hydrogenation. Figure 7 refers to the 2.44 fs cell, Figure 9 to the 10 fs cell. In defining dangling bonds we used the above mentioned criteria for the Si-Si; *i.e.*, 2.851 Å in Figure 7, and 2.743 Å in Figure 9. These criteria generated 5 and 2 dangling bonds respectively, confirming that the longer time-step simulation generated a more saturated structure.

For the hydrogenated samples we took the cut-off radius for a Si-H bond to be 1.9 Å. This is the position of the minimum between the first and second peaks in the Si-H partial RDF. Figures 8 and 10 show what happened upon hydrogenation. In the 2.44/0.46 simulation, 3 bonds were passivated by hydrogen, 2 disappeared by the closing up of Si atoms and 3 new dangling bonds appeared. In the 10/2 simulation, only 1 bond was passivated by a hydrogen atom, 1 closed due to the motion of the Si atoms and 2 new dangling bonds appeared. Again, the fact that the

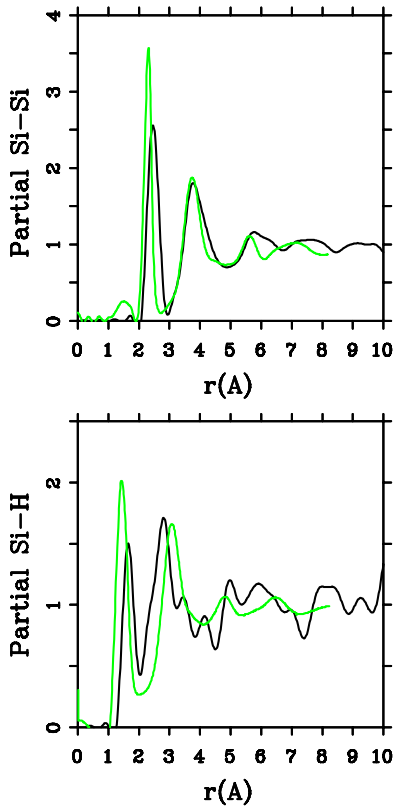

Fig. 11. Partial Si-Si and Si-H RDFs for the hydrogenated 2.44/0.46 cell. The dark lines are our simulation and the light lines are the experimental results.

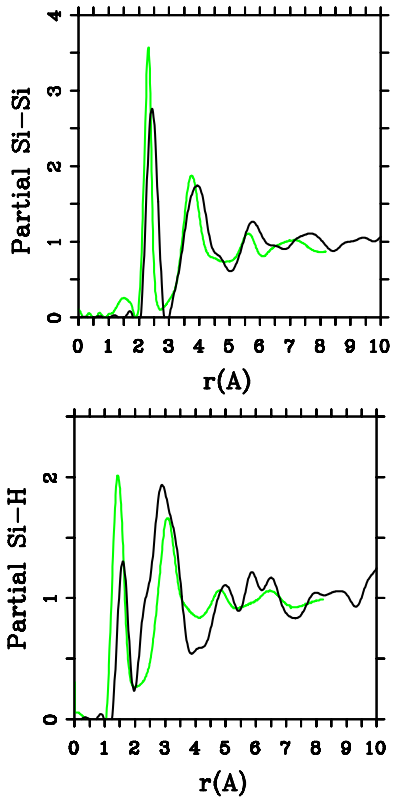

Fig. 12. Partial Si-Si and Si-H RDFs for the hydrogenated 10/2 cell. The dark lines are our simulation and the light lines are the experimental results.

total number of dangling bonds was the same in the unhydrogenated and hydrogenated confirms the saturated nature of the original sample and explains why di-hydrogen was formed. The RDFs for Si-Si and Si-H are shown in Figure 11 for the 2.44/0.46 cell, and in Figure 12 for the 10/2 cell, along with the measured partials (see [17]). The overall agreement between the experimental and simulated Si-Si and Si-H partial RDFs is quite reasonable as the direct comparison indicates. In this case, there is no strong distinction between the two simulations. Thus the most sensitive probe of the structure of the hydrogenated sample is, as one expects, the H-H partial RDF.

4.2 The electronic density of states

An analysis of structural defects *versus* spectral defects, performed by Drabold *et al.* [24], led to the conclusion that dangling bonds give rise to defects within the gap, and that some strained tetrahedral structures may also generate gap states, but that floating bonds do not create gap states. More recent work, however, indicates that floating bonds may generate gap states [49] and this conclusion is also borne out in the results reported here on the basis of Γ-point calculations of the electronic density of states (DOS). Makov *et al.* [50], in particular, have focused on potential problems when calculating total energies using a single k-point located at Γ. As an example, they performed a calculation of the energy of the ideal vacancy defect in silicon, a system that has been studied extensively and was believed to require supercells with as many as 200 atoms for convergence. However, it was found that a 60-atom periodic supercell calculation with a single k-point at Γ gave a result practically identical to that obtained using 864 k-points and a 16-atom fcc supercell. This calculation is believed to give the defect energy to an accuracy of better than 0.1 eV. While not conclusive in terms of computations of the electronic structure and DOS, this calculation does support use of Γ-point sampling in the present calculations.

Γ-point calculations of the electronic density of states are a widespread practice in the field. Consistent with this practice DOS curves were obtained by broadening the discrete eigenvalue spectra generated using the final amorphous structures. Results were obtained using the overlapped atom potential construction of *FastStructure*, and using the self-consistent eigenvalue spectra in *DMol3*. All computations were performed within the LDA approximation.

For *a*-Si two cells were constructed, we recall, using the crystalline density, one with a 2.44 fs time step and another with a 10 fs time step. The short time step cell has 5 dangling bonds (dbs) and 5 floating bonds (fbs), whereas the long time step cell has 2 dbs and 2 fbs for cutoff radii of 2.763 and 2.7716 Å, respectively; at these distances the number of first neighbors (area under the first

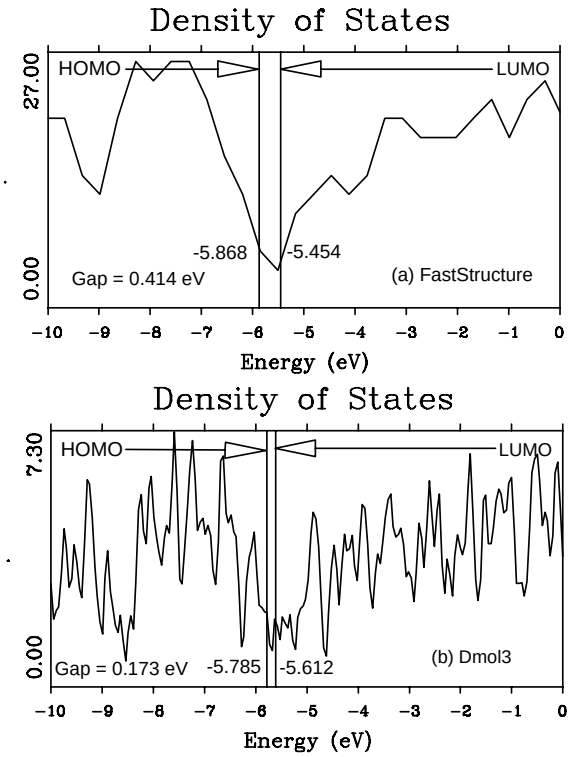

Fig. 13. DOS curves for the 2.44 fs cell of *a*-Si calculated using *FastStructure*, curve (a), and *DMol3*, curve (b). HOMOs, LUMOs and gaps are indicated.

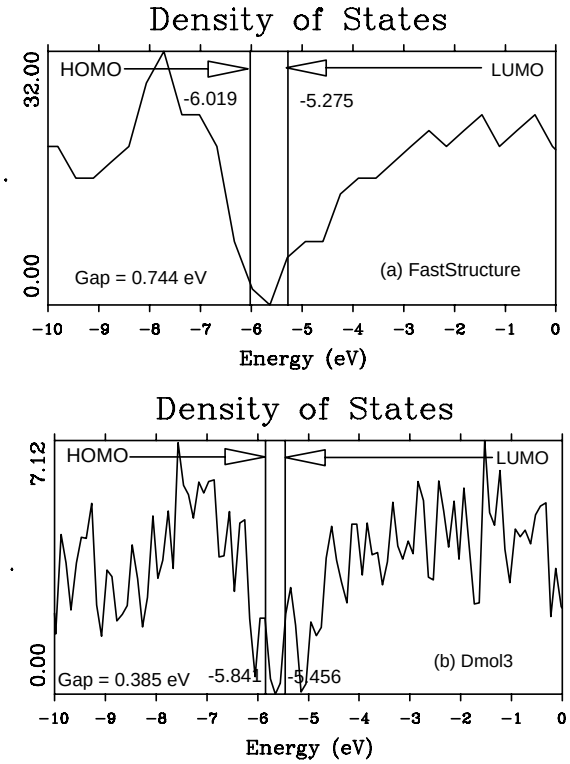

Fig. 14. DOS curves for the 10 fs cell of *a*-Si calculated using *FastStructure*, curve (a), and *DMol3*, curve (b). HOMOs, LUMOs and gaps are indicated.

amorphous peak) is equal to 4. Calculations of the DOS curves, and HOMOs (highest occupied molecular orbitals) and LUMOs (lowest unoccupied molecular orbitals) with both *FastStructure* and *DMol3* for the 2.44 fs and 10 fs cells simulating pure *a*-Si gave the DOS shown in Figures 13 and 14. For the DOS curves obtained with *FastStructure* the discrete spectra was broadened with 0.02 eV half-width Gaussians, and for those obtained with *DMol3* the σ used was 0.05 eV.

The gaps were obtained as the difference LUMO-HOMO with no attempt made to sort out the states within or near the gap due to dbs and/or fbs. The 2.44 fs cell displayed a smaller gap than the 10 fs cell, consistent with an inhibiting of the size of the gap with increasing defect density. This is of course expected, because the larger defect density presumably creates more 'gap states' and so would normally reduce the overall HOMO-LUMO splitting. The numbers were potential dependent — 0.414 eV *vs.* 0.744 eV using *FastStructure* and 0.173 eV *vs.* 0.385 eV using *DMol3*, but the sign was consistent with a narrower gap in the sample with the higher defect density.

The two *a*-Si:H cells (which, we recall, were constructed using a hydrogenated density of 2.2 g/cm^3 and are identified by the time steps as 2.44/0.46 and 10/2) gave rise to the DOS shown in Figures 15 and 16. Again, results are shown for the overlapped atom potential of *FastStructure* and the fully self-consistent potential of *DMol3*. As can be seen, hydrogenation reduces the size of the gap for the 2.44/0.46 cell from 0.414 eV to 0.324 eV (over-

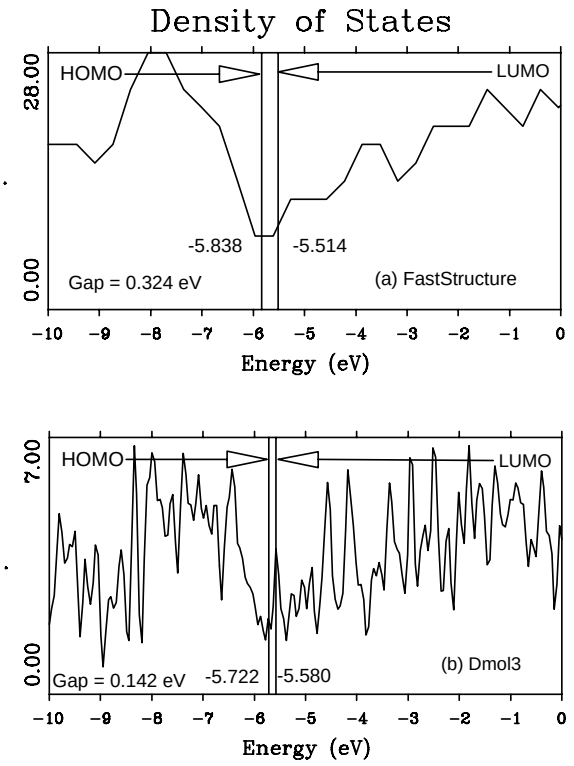

Fig. 15. DOS curves for the 2.44/0.46 fs cell of *a*-Si:H calculated using *FastStructure*, curve (a), and *DMol3*, curve (b). HOMOs, LUMOs and gaps are indicated.

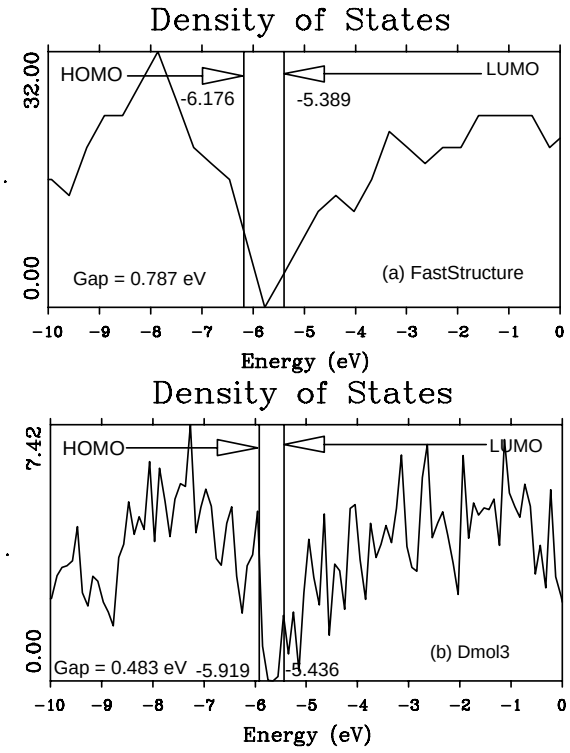

Fig. 16. DOS curves for the 10/2 fs cell of *a*-Si:H calculated using *FastStructure*, curve (a), and *DMol3*, curve (b). HOMOs, LUMOs and gaps are indicated.

lapped atom potential) and from 0.17 eV to 0.14 eV for the self-consistent potential. This sample has 3 dbs and a large number of floating bonds, 11 (6 hydrogen related and 5 silicon related) indicating the important role of the floating bonds in reducing the gap. For the 10/2 cell the size of the gap increases from 0.74 to 0.79 eV (overlapped atoms) and from 0.38 to 0.48 eV (self-consistent). This cell has 2 dbs and 3 fbs. An increase of the gap is also observed experimentally.

5 Conclusions

In attempting to generate *via* computer simulations samples of the likely atomic arrangements in amorphous samples of covalent semiconductors, a compromise is needed. Use of a simple force-field allows simulations over long times and with large samples to be carried out. However, the generation of force-fields that describe the interactions with sufficient accuracy is time consuming and system specific. On the other hand, when quantum methods are used to generate the forces, one has the advantage of universality, but is unable to carry out simulations for long times and for large samples.

In the present work, we used quantum forces generated by a fast method (*via* use of the Harris Functional and *FastStructure*) and a simulation protocol that is different from the standard procedure. The protocol consists of heating a crystalline sample of 64 atoms of silicon to just below its melting temperature and then cooling it down to 0 K with subsequent annealing and quenching cycles at temperatures dictated by experiment. This protocol was found to generate amorphous samples with fewer dangling bonds and fewer overcoordinated defects than standard protocols and generated structures having total and partial radial distribution functions whose main features lined up well with measurements performed on *a*-Si and *a*-Si:H. In the hydrogenated samples, the hydrogen atoms were not placed in position as has sometimes been done, but were allowed to move freely through the cell and quench into low energy configurations. Where dangling bonds were available, the hydrogens tended to attach there. In the absence of a sufficient defect concentration, di-hydrogen tended to form.

The electronic density of states showed expected behaviour as regards the influence of defects. On hydrogenation of a low defect density sample, the gap was found to increase, as is found experimentally. For the high defect density on the other hand, the gap decreased; we believe due to the high number of existing floating bonds. Of course, it is possible that this behaviour had to do with the specific samples and more work would be necessary to establish a general principle.

The protocol we used to generate amorphous samples is not restricted to *a*-Si and *a*-Si:H but can be used for monatomic or diatomic amorphous semiconducting materials. We expect to report work on amorphous silicon-nitrogen alloys in the near future.

AAV thanks DGAPA-UNAM for financial support to spend a sabbatical year at *Molecular Simulations, Inc.* where this work was begun and for financial support to carry out this research through project IN101798 (*Estructura Electrónica y Topología Atómica de Silicio Amorfo Puro y Contaminado*). FA thanks CONACyT for supporting his PhD studies. We thank A. Menelle for making a copy of his Docteur de L'Université thesis available to us. This work was done on an Origin 2000 computer provided by DGSCA, UNAM.

References

1. G. Szekely, J. Electrochem. Soc. **98**, 318 (1951).
2. H. Richter, G. Breitling, Z. Naturf. **13a**, 988 (1958), and work cited therein.
3. R. Grigorovici, R. Manaila, Thin Solid Films **1**, 343 (1968).
4. M.V. Coleman, D.J.D. Thomas, Phys. Stat. Solidi **25**, 241 (1968).
5. A.A. Valladares, A. Valladares, R.M. Valladares, M.A. Mc Nelis, J. Non-Cryst. Solids **231**, 209 (1998); R.M. Valladares, C.C. Díaz, M. Arroyo, M.A. Mc Nelis, Ariel A. Valladares, Phys. Rev. B **62**, 2220 (2000).
6. N.F. Mott, E.A. Davis, *Electronic Processes in Non-crystalline Materials* (Oxford University Press, 1971), p. 272

7. W.E. Spear, P.G. Le Comber, Solid State Commun. **17**, 9 (1975).
8. R.A. Street, *Hydrogenated Amorphous Silicon* (Cambridge University Press, 1991).
9. T.A. Postol, C.M. Falco, R.T. Kampwirth, I.K. Schuller, W.B. Yelon, Phys. Rev. Lett. **45**, 648 (1980).
10. S.C. Moss, J.F. Graczyk, Phys. Rev. Lett. **23**, 1167 (1969), and *Proceedings of the 10th International Conference on the Physics of Semiconductors*, edited by S.P. Keller, J.C. Hensel, F. Stern (Cambridge, 1970, United States Atomic Energy Comission), p. 658.
11. A. Barna, P.B. Barna, G. Radnóczi, L. Tóth, P. Thomas, Phys Stat. Sol. A **41**, 81 (1977).
12. R. Mosseri, C. Sella, J. Dixmier, Phys. Stat. Sol. A **52**, 475 (1979).
13. J. Fortner, J.S. Lannin, Phys. Rev. B **39**, 5527 (1989).
14. S. Kugler, G. Molnár, A. Menelle, Phys. Rev. B **40**, 8030 (1989).
15. S. Kugler, L. Pustai, L. Rosta, Phys. Rev. B **48**, 7685 (1993).
16. K. Laaziri, S. Kycia, S. Roorola, M. Chicoine, J.L. Robertson, J. Wang, S.C. Moss, Phys. Rev. Lett. **82**, 3460 (1999).
17. R. Bellissent, A. Chenevas-Paule, P. Chieux, A. Menelle, J. Non-Cryst. Solids **77-78**, 213 (1985).
18. R. Bellissent, A. Menelle, W.S. Howells, A.C. Wright, T.M. Brunier, R.N. Sinclair, F. Jansen, Physica B **156-157**, 217 (1989).
19. J.L. Feldman, S.R. Bickham, G.E. Engel, B.N. Davidson, Phil. Mag. B **77**, 507 (1998).
20. E. Roger Cowley, Phys. Rev. Lett. **60**, 2379 (1988). See also D.A. Drabold, P.A. Fedders, A.E. Carlsson O.F. Sankey, J.D. Dow, Phys. Rev. B **42**, 5345 (1990).
21. I. Kwon, R. Biswas, C.Z. Wang, K.M. Ho, C.M. Soukoulis, Phys. Rev. B **49**, 7242 (1994).
22. Q. Li, R. Biswas, Phys. Rev. B **50**, 18090 (1994).
23. R. Car, M. Parrinello, Phys. Rev. Lett. **60**, 204 (1988).
24. D.A. Drabold, P.A. Fedders, O.F. Sankey, J.D. Dow, Phys. Rev. B **42**, 5135 (1990).
25. I. Stich, R. Car, M. Parrinello, Phys. Rev. B **44**, 11092 (1991).
26. P.A. Fedders, D.A. Drabold, S. Klemm, Phys. Rev. B **45**, 4048 (1992).
27. F. Wooten, K. Winer, D. Weaire, Phys. Rev. Lett. **54**, 1392 (1985).
28. I. Lee, K.J. Chang, Phys. Rev. B **50**, 18083 (1994).
29. F. Buda, G.L. Chiarotti, R. Car, M. Parrinello, Phys. Rev. B **44**, 5908 (1991).
30. P.A. Fedders, D.A. Drabold, Phys. Rev. B **47**, 13277 (1993).
31. B. Tuttle, J.B. Adams, Phys. Rev. B **53**, 16265 (1996).
32. O.F. Sankey, D.J. Niklewsky, Phys. Rev. B **40**, 3979 (1989), O.F. Sankey, D.A. Drabold, Bull. Am. Phys. Soc. **36**, 924 (1991).
33. J. Harris, Phys. Rev. B **31**, 1770 (1985).
34. R. Biswas, C.Z. Wang, C.T. Chan, K.M. Ho, C.M. Soukoulis, Phys. Rev. Lett. **63**, 1491 (1989).
35. P.A. Fedders, J. Non-Cryst. Solids **137&138**, 141 (1991).
36. L. Colombo, D. Maric, Europhys. Lett. **29**, 623 (1995).
37. R. Yang, J. Singh, J. Non-Cryst. Solids **240**, 29 (1998).
38. P. Klein, H.M. Urbassek, T. Frauenheim, Phys. Rev. B **60**, 5478 (1999).
39. *Tight-Binding Approach to Computational Materials Science*, edited by P.E.A. Turchi, A. Gonis, L. Colombo, *MRS Symposium Proceedings, Vol. 491, 1998* (Materials Research Society, Warrendale PA., USA).
40. *FastStructure_SimAnn, User Guide*, Release 4.0.0 (San Diego, Molecular Simulations, Inc., September 1996).
41. Xiao-Ping Li, J. Andzelm, J. Harris, A.M. Chaka, *Chemical Applications of Density-Functional Theory*, edited by B.B. Laird, R.B. Ross, T. Ziegler (American Chemical Society, Washington, DC, 1996), Chap. 26.
42. S.H. Vosko, L. Wilk, M. Nusair, Can. J. Phys. **58**, 1200 (1980).
43. Z. Lin, J. Harris, J. Phys. Cond. Matt. **5**, 1055 (1992).
44. B. Delley, J. Chem. Phys. **92**, 508 (1990).
45. P. Hohenberg, W. Kohn, Phys. Rev. B **136**, 864 (1964).
46. W. Kohn, L.J. Sham, Phys. Rev. A **140**, 1133 (1965).
47. *Quantum Chemistry, DMol3 User Guide*, Cerius2-3.5 (Molecular Simulations, Inc., San Diego, 1996). See also B. Delley, J. Chem. Phys. **92**, 508 (1990); **94**, 7245 (1991).
48. K.G. Nakamura, K. Ishioka, M. Kitajima, K. Murakami, Solid State Comm. **101**, 735 (1997).
49. M. Fornari, M. Peressi, S. de Gironcoli, A. Baldereschi, Europhys. Lett. **47**, 481 (1999).
50. G. Makov, R. Shah, M.C. Payne, Phys. Rev. B **53**, 15513 (1996).